

Induced vanadium polarization in intermetallic iron based compounds: XMCD and *ab initio* study

M.G. SHELYAPINA^{1*}, N.E. SKRYABINA², D. FRUCHART³, E.K. HLIL³, P. WOLFERS³, J. TOBOŁA⁴

¹ V.A. Fock Institute of Physics, St. Petersburg State University,
Ulyanovskaya St. 1, Petrodvorets, 198504 St. Petersburg, Russia

² Faculty of Physics, Perm State University, Bukireva St. 15, 614990 Perm, Russia

³ MCMF, Institut Néel, CNRS, BP 166, 38042 Grenoble cedex 9, France

⁴ Faculty of Physics and Applied Computer Science, AGH University of Science and Technology,
Al. Mickiewicza 30, 30 059 Krakow, Poland

* Corresponding author. E-mail: marinashelyapina@mail.ru

Received February 15, 2008; accepted February 17, 2008; available on-line March 31, 2008

The vanadium magnetic polarization in NdFe_{12-x}V_x and Fe_{1-x}V_x intermetallic compounds has been studied by X-ray magnetic circular dichroism. For all the compounds it was found that the vanadium moment is always antiferromagnetically coupled with the iron moment and reaches the value of 1 μ_B for systems with low vanadium concentration. A theoretical KKR-CPA study of hyperfine fields in Fe_{1-x}V_x revealed the induced character of the vanadium polarization.

Iron-based alloys / X-ray magnetic circular dichroism / *Ab initio* calculations

Introduction

It is well known that vanadium metal is generally nonmagnetic. However, onset of magnetism was evidenced for V particles [1]. Later different iron-based intermetallic systems with polarization on vanadium were predicted theoretically and revealed experimentally. A neutron investigation of Fe_{1-x}V_x alloys proved that the magnetic polarization of vanadium could reach 1 μ_B [2,3]. A vanadium polarization of the same order was theoretically predicted for Heusler-type Fe_{3-x}V_xAl alloys [4]. A recent X-ray magnetic circular dichroism (XMCD) analysis of Fe/V multilayers also revealed a significant polarization on V atoms [5]. In this paper we report on an XMCD study of intermetallic iron-based systems such as NdFe_{12-x}V_x and disordered Fe_{1-x}V_x alloys.

It has been observed that NdFe_{12-x}V_x compounds exhibit optimized intrinsic magnetic properties [6-8]. In these 1:12 type compounds (structure type: ThMn₁₂, space group: *I4/mmm* [9]), the Fe sublattice has uniaxial magnetic anisotropy, while that of the rare earth sublattice is planar. Competition of these two anisotropies potentially results in a spin re-orientation transition from planar to axial and from low to high temperatures. For example, for NdFe₁₀V₂, a spin re-orientation was found at 130 K [8]. In 1:12 systems the rare earth atom occupies the 2a position

and the 3d atoms are distributed on three different sites: 8f, 8i, 8j. In NdFe_{12-x}V_x compounds vanadium atoms occupy only the 8i site, the 8j and 8f sites being exclusively occupied by Fe atoms [7].

The bcc Fe_{1-x}V_x alloys can be considered as a simplified model of 1:12 systems in terms of the V-atom coordination, where the influence of the rare earth atoms is neglected.

Experimental and fundamental bases

Sample synthesis and analysis

The Fe_{1-x}V_x alloys ($x = 0.04, 0.08, 0.16$ and 0.2) were prepared by induction melting using the cold crucible technique under purified argon atmosphere. The constituents, Fe (99.99% purity) and V (99.95% purity), were melted, then rapidly cooled down three times successively, thus leading to a complete combination of the metal atoms and a good homogeneity of the samples. The phase analysis and the cell parameters were checked by X-ray investigations using a PW 1720 Philips set-up (Cu K α radiation, backscattering graphite monochromator). The NdFe_{12-x}V_x samples ($x = 1.5, 2, 2.5$) were prepared by induction melting and then annealed under high vacuum at temperatures between 900 and 1050°C in order to stabilize the pure 1:12 phase.

XMCD experiments

XMCD techniques were used to analyze the ferromagnetic components of Fe and V. More particularly those of the atomic orbitals exhibiting a direct or indirect magnetic polarization were checked for, since these techniques are chemically and orbitally selective.

The $L_{2,3}$ edges of iron and vanadium were recorded at different temperatures and in applied magnetic fields using the facilities of the S23 spectrometer installed at the super ACO ring of LURE, Orsay, France. The analysis was made using a polished surface of a bulk sample. The dichroic signals were extracted from the difference of the two absorption curves, when applying successively a reverse magnetizing field (along the photon beam) on the samples. More details on the experimental set-up can be found in the LURE technical handbook [10].

Sum rules

For the $L_{2,3}$ edges of the transition metals, as well as for the $M_{4,5}$ edges of the rare-earth, sum rules can be deduced. We used the sum rules proposed by Thole *et al.* [11] and by Carra *et al.* [12] for atoms, and by Guo *et al.* [13] and Ankudinov and Rehr [14] for solids. Neglecting the dipole operator and combining the rules for expectation values of the angular momentum operator of the d states $\langle L_x \rangle$ and that one of the spin operator $\langle S_z \rangle$, we can obtain the ratio $\langle L_z \rangle / \langle S_z \rangle$. For the $L_{2,3}$ edges of the $3d$ metals ($2p \rightarrow 3d$ transition) it takes the following form

$$\frac{\langle L_z \rangle}{\langle S_z \rangle} = \frac{1}{3} \frac{\int_{L_2+L_3} d\omega [\mu_+(\omega) - \mu_-(\omega)]}{\int_{L_3} d\omega [\mu_+(\omega) - \mu_-(\omega)] - 2 \int_{L_2} d\omega [\mu_+(\omega) - \mu_-(\omega)]} \quad (1)$$

where $\mu_{\pm}(\omega)$ and $\mu_0(\omega)$ are the absorption coefficients for polarized and nonpolarized X-ray radiation, respectively. Combining this ratio with the

magnetic moment obtained from neutron measurements, that is

$$\langle L \rangle = \langle L_z \rangle + 2 \langle S_z \rangle \quad (2)$$

we can determine completely $\langle L \rangle$, $\langle L_z \rangle$ and $\langle S_z \rangle$ [15].

Computational details

For the theoretical study of the $\text{Fe}_{1-x}\text{V}_x$ disordered alloys we applied the spin-polarized Korringa-Kohn-Rostoker method combined with Coherent-Potential-Approximation [16] within the LSDA framework [17] (KKR-CPA). In this method the electron charge density and the crystal potential are assumed to be spherically symmetrical within muffin-tin spheres and constant in the interstitial region. The radii of the muffin-tin spheres were chosen on the one hand not to overlap and on the other hand to improve the fitting of the Wigner-Seitz volume. The total, core, valence and non- s decomposed hyperfine fields calculated for the final potential converged up to 1 mRy. The s -, p - and d -valence states were taken into account [17]. All calculations were carried out using the Munich SPR-KKR package [18]. For the cell parameter of $\text{Fe}_{1-x}\text{V}_x$ we supposed that the lattice parameter varies linearly with x . For more details see [19].

Results and discussion

To have a global picture of the magnetic structure of the $\text{Fe}_{1-x}\text{V}_x$ alloys we recorded and analyzed the $L_{2,3}$ edges of both $3d$ metals. The $L_{2,3}$ Fe and V edges were checked at room temperature with an applied field of 0.9 T versus the vanadium concentration x . Typical X-ray absorption spectra (XAS) at $L_{2,3}$ edges are shown in Fig. 1.

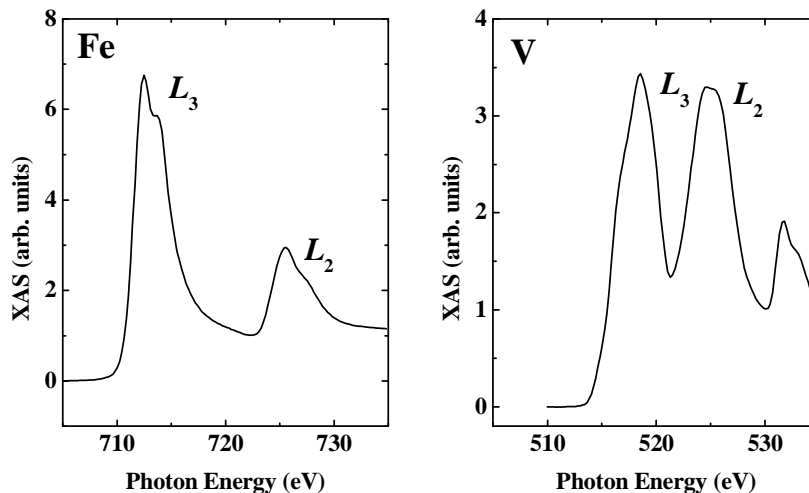


Fig. 1 XAS spectra at the iron and vanadium $L_{2,3}$ edges in the $\text{Fe}_{0.92}\text{V}_{0.08}$ alloy.

For both the Fe and V atoms the L_2 and L_3 edges partly overlap; this is caused by the small spin-orbit splitting of the core states. Such a splitting is found close to 13 eV for Fe and 7 eV for V. The branching ratio of the experimental Fe XAS spectra is 2:1 as for free Fe atoms, while for V the branching ratio is found close to 1:1. This is the usual case for XAS spectra of early 3d metals, where a strong electron-core interaction leads to L_2 and L_3 spectra intermixing [15,16]. Therefore, for V, separation into L_2 and L_3 is under condition. A third peak, at 532 eV, corresponds to the oxygen K_1 edge. Additional small peaks due to the presence of an iron oxide were observed for all studied $\text{Fe}_{1-x}\text{V}_x$ alloys; however, they did not contribute to the XMCD signal.

The XMCD spectra of the $L_{2,3}$ edges for Fe and V in the $\text{Fe}_{1-x}\text{V}_x$ alloys with $x = 0.04, 0.08, 0.16$ and 0.2 are represented in Fig. 2. All spectra were recorded under an applied magnetic field of 0.9 T, which corresponds to the ferromagnetic state with saturated magnetic moment. As one can see, a non-zero 3d magnetic moment of vanadium was found for all compounds. As evidenced from Fig. 2, the vanadium magnetic moment is always opposite to that of iron, a result confirming previous neutron [2] and Mössbauer spectroscopy [3] investigations, as well as more recent XMCD experiments for a $\text{Fe}_{0.9}\text{V}_{0.1}$ alloy [20]. The maximal polarization of both iron and vanadium atoms corresponds to the iron-rich alloys, in fair

agreement with neutron scattering data and our calculations as represented in Fig. 3a.

The calculated orbital contribution to the magnetic moment is shown in Fig. 3b. The orbital magnetic moment is almost quenched for both atoms. For iron the spin to orbit ratio as deduced from the application of the sum rules seems not to change noticeably within the considered vanadium concentration range, see Fig. 4. The theoretical $\langle L_z \rangle / \langle S_z \rangle$ value estimated from the KKR-CPA calculations confirmed roughly the general trends of the experimental variation. For V such an analysis was not made. Due to the strong electron core-hole interaction, the treatment of the XMCD spectra is rather complicated and application of the sum rules is questionable.

In order to better understand the origin of the magnetic polarization on vanadium in $\text{Fe}_{1-x}\text{V}_x$ we calculated the hyperfine fields B_{hf} on both Fe and V atoms versus the vanadium concentration x . The total, core, valence and non- s contributions to B_{hf} are shown in Fig. 5. As evidenced from the calculations, the vanadium polarization is completely induced by surrounding iron atoms.

The experimental XMCD spectra of $\text{NdFe}_{12-x}\text{V}_x$ ($x = 1.5, 2$ and 2.5) as recorded at different temperatures at the $L_{2,3}$ edges of iron and vanadium are shown in Fig. 6. The shape of the XAS and XMCD signals in the $\text{NdFe}_{12-x}\text{V}_x$ compounds are similar to those obtained for binary $\text{Fe}_{1-x}\text{V}_x$ alloys. As for the Fe-V

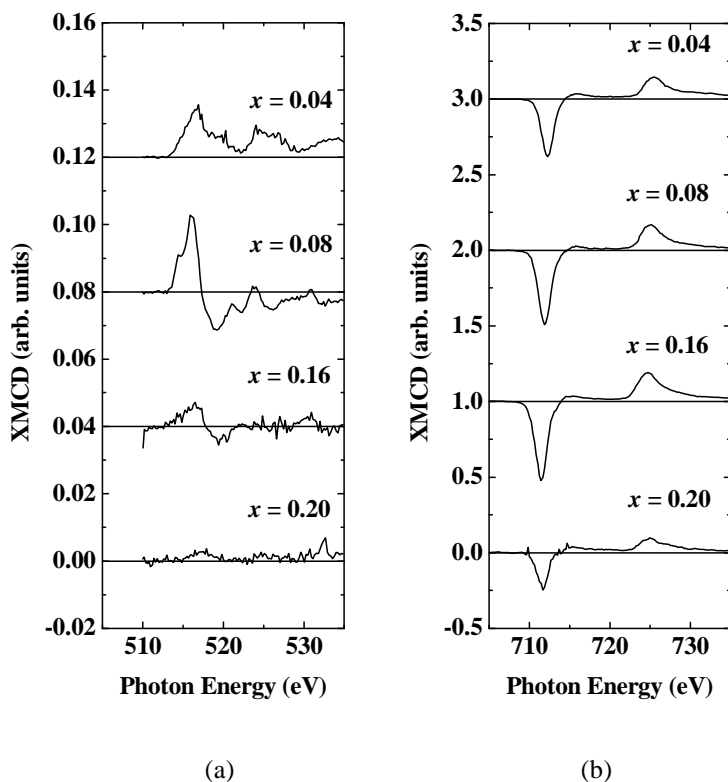
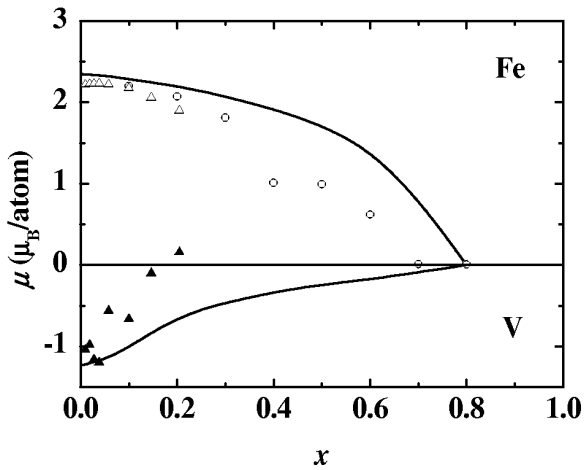
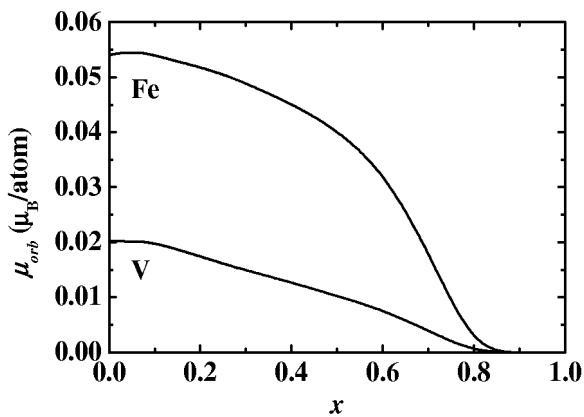


Fig. 2 XMCD signal at the $L_{2,3}$ edges of iron (a) and vanadium (b) in $\text{Fe}_{1-x}\text{V}_x$ for different x values, for $T = 250$ K, under $H = 0.9$ T.



(a)



(b)

Fig. 3 KKR-CPA V and Fe magnetic moments in $Fe_{1-x}V_x$ versus V concentration x : total atomic moments (a), orbital contribution (b). Experimental data are given as well (triangles – Ref. [2], circles – Ref. [3]).

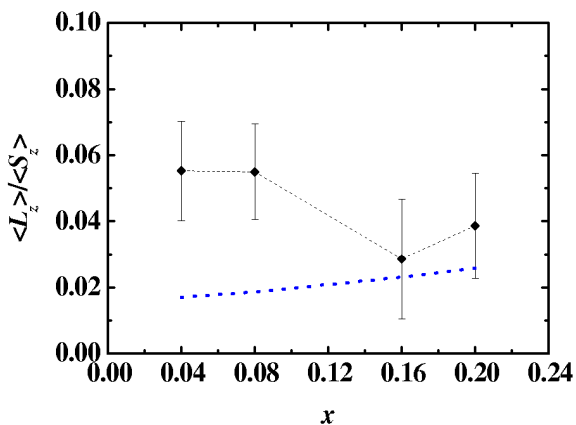
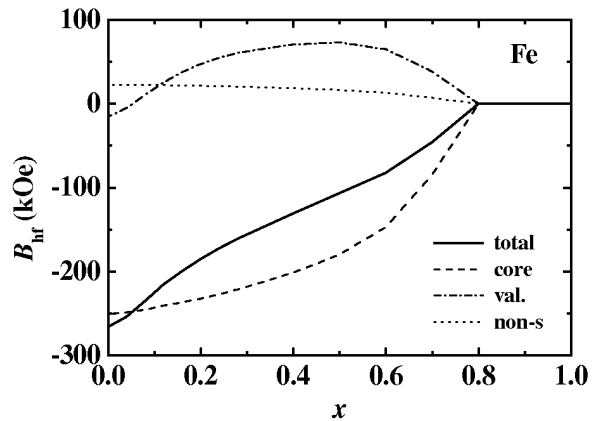
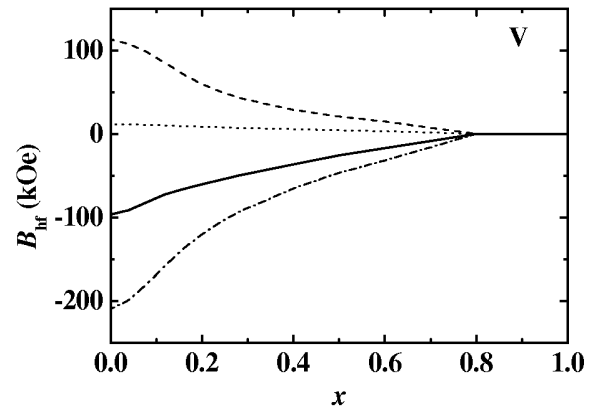


Fig. 4 $\langle L_z \rangle / \langle S_z \rangle$ ratio for Fe in $Fe_{1-x}V_x$ versus vanadium concentration x obtained from XMCD spectra at the $L_{2,3}$ edges of iron; the continuous line is a guide of the eye. Calculated values are shown by a dashed line.



(a)



(b)

Fig. 5 Total, core, valence and non- s contributions to the calculated hyperfine fields on Fe (a) and V (b) in $Fe_{1-x}V_x$.

system, the V and Fe $3d$ moments are antiparallel. As one can see from Fig. 6, at low temperature the XMCD signals for both Fe and V are maximal for the intermediate compound with $x = 2$. For Fe, with increasing temperature the XMCD signal at first decreases, being at $T = 80$ K a third of its value at $T = 10$ K, and then increases again. For V, the XMCD signal at 150 K remains similar to that measured at 80 K. For the $L_{2,3}$ edges of iron the sum rules were applied; the temperature dependence of $\langle L_z \rangle / \langle S_z \rangle$ is presented in Fig. 7. The anomalous behavior of the $\langle L_z \rangle / \langle S_z \rangle$ ratio for $x = 1.5$ and 2 versus temperature (minimum close to 75 K) should be correlated with a spin reorientation process, as evidenced by neutron diffraction experiments [7]. Under this consideration the results presented in Figs. 6 and 7 will be discussed in more details in a forthcoming paper.

Conclusion

X-ray magnetic circular dichroism and *ab initio* KKR-CPA calculations are efficient to establish the presence of an induced magnetic polarization on vanadium. For the systems considered here, it was

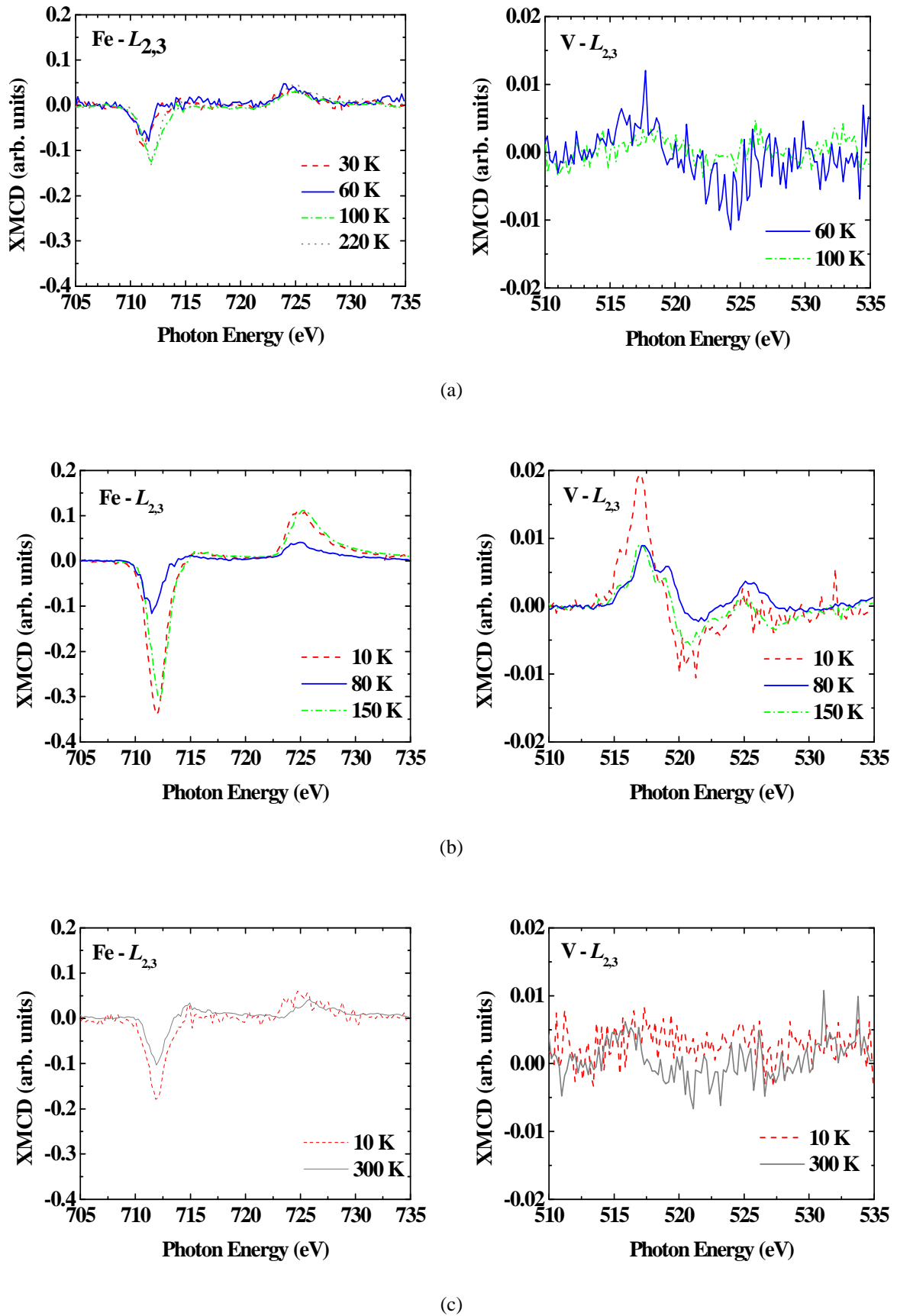


Fig. 6 XMCD spectra at the $L_{2,3}$ edges of iron (left) and $L_{2,3}$ edges of vanadium (right) in $\text{NdFe}_{12-x}\text{V}_x$ with $x = 1.5$ (a), 2 (b) and 2.5 (c).

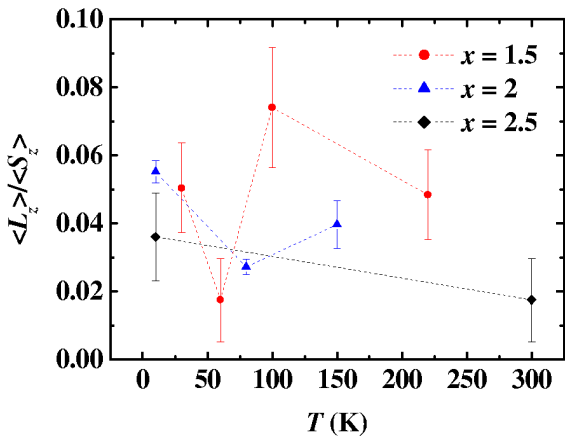


Fig. 7 Temperature dependencies of the $\langle L_z \rangle / \langle S_z \rangle$ ratio in NdFe_{12-x}V_x compounds for different x values, obtained from XMCD spectra at the $L_{2,3}$ edges of iron.

found that the vanadium moment is antiparallel to that of iron. KKR-CPA calculations for Fe_{1-x}V_x disordered alloys revealed that the V magnetic moment is completely induced by Fe atoms and reaches 1 μ_B for low vanadium concentrations. In a forthcoming paper we will report the results of the XMCD study of the Nd magnetic polarization in NdFe_{12-x}V_x together with theoretical calculations of its magnetic structure.

Acknowledgements

This work was supported by the ECO-NET programme under the project No 081 33 RA and by the Russian Foundation for Basic Research under the grant No 05-02-16731-a.

References

- [1] H. Akoh, A. Tasaki, *J. Phys. Soc. Jpn.* 42 (1977) 791.
- [2] I. Mirebeau, M.C. Cadeville, G. Parette, I.A. Campbell, *J. Phys. F: Metal Physics* 12 (1982) 25.
- [3] J.C. Krause, J. Schaf, M.I. da Costa Jr, C. Paduani, *Phys. Rev. B* 61 (2000) 6196.
- [4] A. Bansil, S. Kaprzyk, P.E. Mijnaerends, J. Toboła, *Phys. Rev. B* 60 (1999) 13396.
- [5] G.R. Harp, S.P. Parkin, W.L. O'Braien, B.P. Tonner, *Phys. Rev. B* 51 (1995) 3293.
- [6] I. Popa, *Ph.D. Thesis*, University J. Fourier, Grenoble, France, 2003.
- [7] I. Popa, D. Fruchart, P. de Rango, S. Rivoirard, P. Wolfers, *J. Magn. Magn. Mater.* 272-276 (2004) 539.
- [8] B.-P. Hu, Y.-Z. Wang, K.-Y. Wang, G.-C. Liu, W.-Y. Lai, *J. Magn. Magn. Mater.* 140-144 (1995) 1023.
- [9] J.V. Florio, N.C. Baenziger, R.E. Rundle, *Acta Crystallogr.* 9 (1956) 367.
- [10] *Technical User's Handbook (Guide Technique)*, LURE, Orsay, France, 1992.
- [11] B.T. Thole, P. Carra, F. Sette, G. van der Laan, *Phys. Rev. Lett.* 68 (1992) 1943.
- [12] P. Carra, B.T. Thole, M. Altarelli, X. Wang, *Phys. Rev. B* 70 (1993) 694.
- [13] G.Y. Guo, H. Ebert, W.M. Temmerman, P.J. Durham, *Phys. Rev. B* 50 (1994) 3861.
- [14] A. Ankudinov, J.J. Rehr, *Phys. Rev. B* 51 (1995) 1282.
- [15] M.G. Shelyapina, M. Morales, M. Bacmann, F. Baudlet, D. Fruchart, C. Giorgetti, E.K. Hlil, G. Krill, P. Wolfers, *J. Alloys Compd.* 383 (2004) 152.
- [16] M. Schröter, H. Ebert, H. Akai, P. Entel, E. Hoffmann, G.G. Reddy, *Phys. Rev. B* 52 (1995) 188-209.
- [17] A.H. MacDonald, S.H. Vosko, *J. Phys. C* 12 (1979) 2977.
- [18] *The Munich SPR-KKR package, v. 2.1*, H. Ebert et al., <http://olymp.cup.uni-muenchen.de/ak/ebert/SPRKKR>; H. Ebert, in: H. Dreyssé (Ed.), *Electronic Structure and Physical Properties of Solids, Lecture Notes in Physics*, Vol. 535, Springer, Berlin, p. 191.
- [19] M.G. Shelyapina, D. Fruchart, E.K. Hlil, N. Skryabina, J. Tobola, P. Wolfers, *J. Alloys Compd.* 383 (2004) 157.
- [20] A. Scherz, H. Wende, K. Baberschke, J. Mínar, D. Benea, H. Ebert, *Phys. Rev. B* 66 (2002) 184401.

Proceeding of the IX International Conference on Crystal Chemistry of Intermetallic Compounds, Lviv, September 20-24, 2005.